

8th International Topical Meeting on Neutron Radiography, Beijing, China, 4-8 September 2016

Visualization of solidification process in lead-bismuth eutectic

Daisuke Ito^{a*}, Yasushi Saito^a, Hiroataka Sato^b, Takenao Shinohara^c

^aResearch Reactor Institute, Kyoto University, 2-1010 Asashironishi, Kumatori, Sennan, Osaka 590-0494, Japan

^bHokkaido University, Sapporo, Japan

^cJ-PARC center, JAEA, Ibaraki, Japan

Abstract

Pulsed neutron transmission spectroscopy was applied to clarify a phase change phenomena of lead-bismuth eutectics (LBE). The melting and solidification behaviors of the LBE should be well understood to enhance the safety of an LBE-cooled accelerator driven system. In this study, the heating experiments were performed using a rectangular test section and LBE phase change process was visualized by the energy-resolved pulsed neutron imaging at BL22 RADEN facility in J-PARC and the solid/liquid interface was identified from the radiograph and Bragg edge information. The transient location of the interface was compared with measured temperature profiles and it would be useful to evaluate the LBE thermal properties.

© 2017 The Authors. Published by Elsevier B.V. This is an open access article under the CC BY-NC-ND license (<http://creativecommons.org/licenses/by-nc-nd/4.0/>).

Peer-review under responsibility of the organizing committee of ITMNR-8

Keywords: Lead-bismuth eutectic,

1. Introduction

Lead-bismuth eutectic (LBE) is a promising candidate of the coolant for accelerator driven system (ADS), because the LBE has high thermal conductivity, low melting temperature, high boiling temperature and chemical stability (Zhang, 2014). In order to establish the safety measure for the LBE-cooled ADS, a lot of studies on thermal hydraulics (natural/forced convection and its heat transfer characteristics) and corrosion effect of the LBE have been carried out. The corrosion of the structural material is an important issue in developing the ADS and the corrosive nature should be investigated in view of material stability and also severe accident conditions. In the LBE flow loop,

* Corresponding author. Tel.: +81-72-451-2373; fax: +81-72-451-2431.

E-mail address: itod@rri.kyoto-u.ac.jp

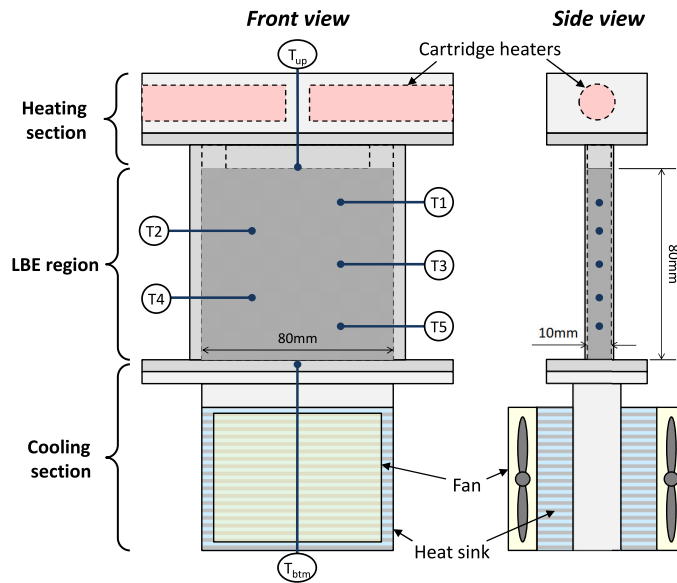


Fig. 1. Experimental setup for LBE heating experiments.

corrosion product is produced in the high temperature region (e.g. reactor core) and transferred to the cold region (e.g. heat exchanger). So, the corrosion product is accumulated in the cold region and might lead to plug formation in the flow channel, resulting in a core-meltdown accident. To prevent such accident due to the coolant blockage, an LBE solidification process with/without corrosion products must be investigated (Agostini, et al., 2004, Zucchini, et al., 2004).

Generally, the phase change characteristics between solid and liquid can be studied analytically by solving the heat conduction equations, so-called Stefan problem. The accurate physical and thermal properties should be given in order to solve such problem. However, these properties for the solid LBE have not been clarified completely, because the crystal structure in solid state affects the thermal properties (Khairulin, et al., 2005; NEA, 2015). Therefore, the material structure and thermal characteristics should be investigated simultaneously.

The present study applies a pulsed neutron transmission spectroscopy to study the LBE solidification process. The crystal structure can be investigated from the Bragg edges appearing in the neutron transmission spectrum (Takada, et al., 2010). So it might be available to clarify the solid-liquid phase change behavior of the LBE using the pulsed neutron imaging technique. In addition, the solid-liquid interface can be identified by using a position sensitive neutron detector. In this study, the neutron imaging experiments of the LBE were performed at BL22 facility in J-PARC and the transient processes of the solidification of the LBE were visualized and analyzed. Finally, the solid-liquid interface was specified from the measured data.

2. Experimental setup and method

2.1. Experimental setup

A schematic diagram of a test section is illustrated in Fig. 1. The LBE sample was encapsulated in a rectangular vessel and sealed. The walls of the test section have 1 mm thickness and were made of stainless steel which has similar thermal conductivity with the LBE. The volume of the confined LBE was $80 \times 80 \times 10 \text{ mm}^3$. The LBE vessel was covered by thermal insulator to prevent the heat loss. In order to decrease the influence of the convection of the liquid phase, the heating section was placed on top vessel and the cooling one was placed at the bottom. The

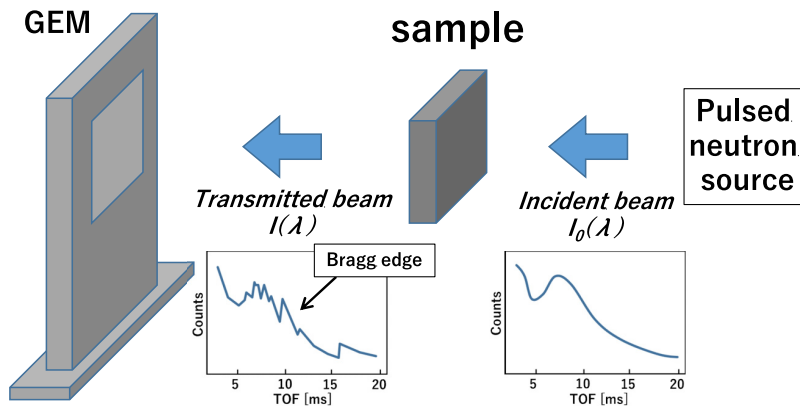


Fig. 2. Pulsed neutron transmission spectroscopy using a GEM detector.

heating and cooling sections were made of aluminum. In the heating section, two cartridge heaters were inserted and the power was controlled by a temperature controlling unit. Two heat sinks with fans were used in the cooling section. Five thermocouples were inserted from the side walls of the vessel, as shown in Fig.1, and the axial temperature profiles in the LBE region were measured with a sampling frequency of 1Hz. Also, the temperatures at the upper and lower walls were recorded.

2.2. Neutron imaging method

The schematic diagram of the pulsed neutron transmission spectroscopy with a position sensitive detector is shown in Fig. 2. Experiments were performed at BL22 RADEN facility in J-PARC. This facility is dedicated to energy selective pulsed neutron transmission imaging and has been applied to a lot of imaging studies on Bragg edge, resonance absorption and polarization of the neutrons. The test section was installed in a front of the detector. The L/D is about 1,000. In the present experiments, a GEM detector (nGEM, Bee Beans Technologies Co., Ltd.) was used to get two-dimensional distributions of time-of-flight (TOF) information. The spatial resolution of this detector is 0.8 mm/pixel and the imaging area is 100 x 100 mm². The wavelength resolution is $\Delta\lambda/\lambda=0.25\%$. Bragg edges, which arise from crystal structure in the material (Sato, et al., 2011), were observed during the phase change of the LBE in the neutron transmission spectrum in each pixel.

3. Results and discussion

Typical histories of the measured temperatures (at upper and lower walls and inside the test section) during the experiment are shown in Fig. 3. The LBE sample was heated from the upper wall for 1 hour (A), and then the upper wall temperature was kept at 220 °C for 1 hour (B). In this situation, the temperature of the upper region in the test section exceeds over the melting point of the LBE ($T_{melt} = 124.7$ °C) and the bottom region was still at lower temperature. As a result, the liquid-solid interface is in the test section. After that, the heating output was stopped and the sample was cooled gradually from the bottom using the cooling fan(C). Finally, all temperatures were below the melting point and the LBE sample was solidified in the test section.

The neutron transmission characteristics for upper and lower parts of the test section in the temperature constant region B is shown in Fig. 4. The total cross-section of the LBE was calculated by the following equation,

$$\Sigma(\lambda) = -\frac{1}{b} \ln \left(\frac{I(\lambda)}{I_0(\lambda)} \right) \quad (1)$$

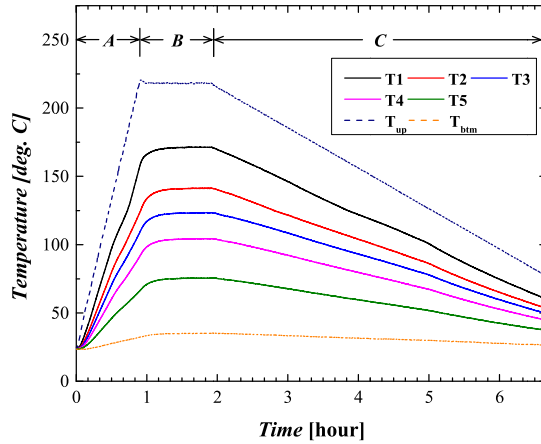
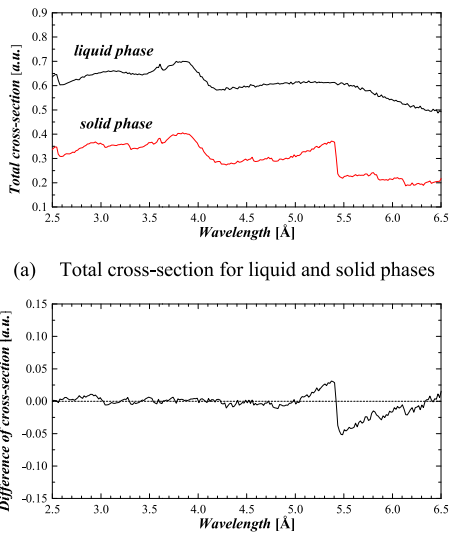


Fig. 3 Temperature transients during the experiment.



(a) Total cross-section for liquid and solid phases
 (b) Difference of cross-section between liquid and solid phases

Fig. 4. Neutron transmission spectra in liquid and solid phases of LBE

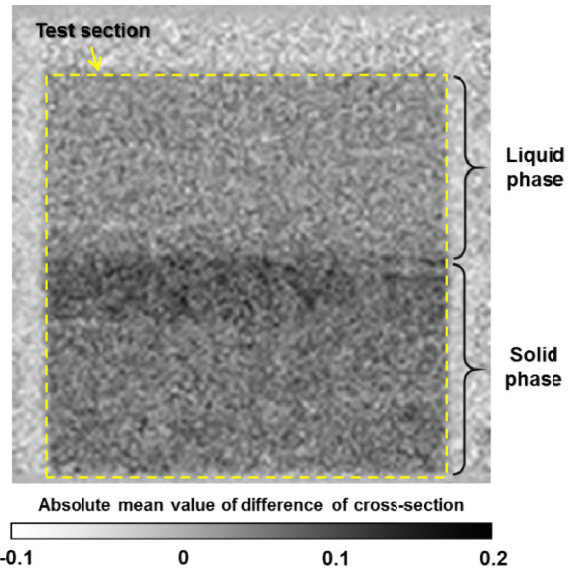


Fig. 5. Wavelength-resolved radiograph ($\lambda=5.0\text{--}6.2 \text{ \AA}$) in B region

where $I(\lambda)$ and $I_0(\lambda)$ are the neutron transmission spectrum with/without the test section, respectively, and b is the thickness of the LBE sample. From this figure, a large Bragg edge can be found in the result of solid phase at $\lambda=5.4 \text{ \AA}$, corresponding to β -phase (101). However, such structural information doesn't appear in the liquid phase. Thus, it is possible to identify the phase state by using this Bragg edge information. Finally, the phase distribution in the temperature constant region B in Fig. 3 could be obtained from the wavelength-resolved radiograph ($\lambda=5.0\text{--}6.2 \text{ \AA}$), as shown in Fig. 5. The difference between liquid and solid phases was clearly visualized. Furthermore, the solid-liquid interface could be specified from the image.

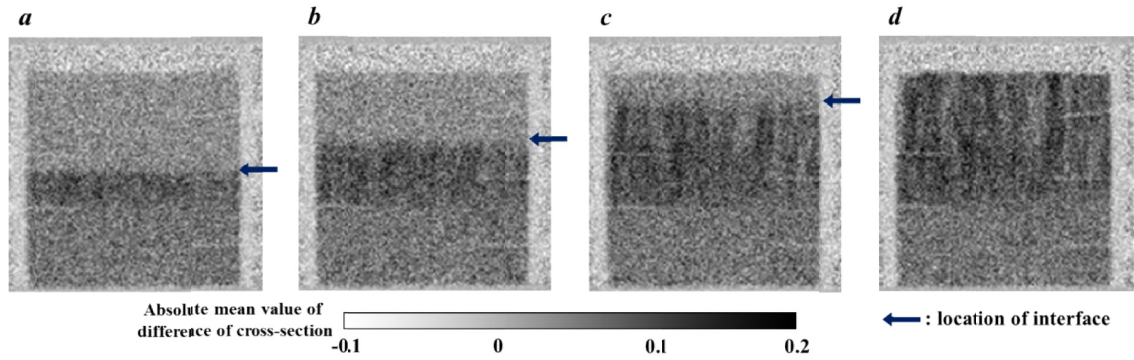


Fig. 6. Temporal change of the wavelength-resolved radiograph in C region, (a) $t=1.92\sim 2.42\text{h}$, (b) $t=2.92\sim 3.42\text{h}$, (c) $t=3.92\sim 4.42\text{h}$, (d) $t=4.92\sim 5.42\text{h}$.

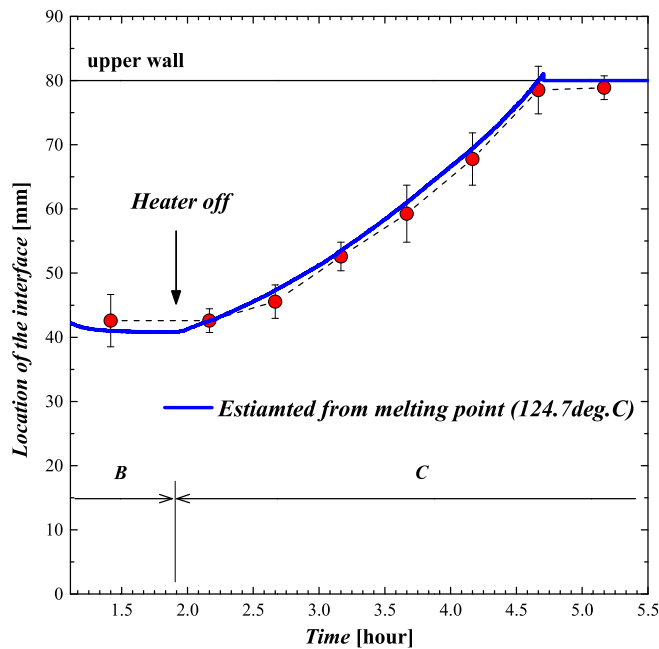


Fig. 7. Transient change of solid-liquid interface location estimated from the neutron transmission radiograph and comparison with measured temperatures

The wavelength-resolved radiographs in C region are shown in Fig. 6. These results are integrated for 30 minutes. The interface could be visualized in each distribution and it moves to upper side by cooling from the bottom. In Fig. 6(d), the interface reached to upper wall and whole sample became the solid state. The difference of the contrast in the solid region is found in these results and might be attributed to the crystal formation in the preparation of the test section. The present setup could not form whole sample melting condition because the heat sink was not insulated during the heating. The LBE in lower half was solidified relatively fast when the test section was prepared at first.

However, in this experiment, the sample was cooled slowly, as shown in Fig. 3. Previously, the difference of the crystal structure due to the solidification speed was reported (Takada, et al., 2010) and so it is expected that the difference in Fig. 6 might be caused by the crystal structure. In addition, there are some striped patterns in the solidified region. It shows a dendrite growth from the coarse structure which exists near the interface at an initial stage of solidification. Such crystal formation can be clarified by observation of solidification with different cooling process.

The location of the interface estimated from the 2D phase distributions is shown in Fig. 7. In B region, the interface is located almost the middle of the test section. After the heater output is stopped, the interface moves upward with time. Finally, the LBE is fully solidified. The solid line in Fig. 7 indicates the interface location estimated from the temperatures measured by the thermocouples in the LBE sample. The solid-liquid interface can be identified using the instantaneous temperature profile and the melting point of the LBE. In the comparison, the result shows good agreement. As a result, the pulsed neutron transmission spectroscopy could be successfully applied to investigate the LBE phase change process.

4. Conclusion

The solid-liquid phase distribution of the LBE was visualized by the pulsed neutron transmission spectroscopy. The experiments were performed at BL22 RADEN facility in J-PARC. The two-dimensional neutron transmission spectra of the LBE were obtained by the GEM detector. The interface between liquid and solid phases of the LBE was identified from the two-dimensional distribution of the transmitted pulsed neutron spectrum. These results will be useful to evaluate the uncertain properties of the LBE, which is very important to analyze the LBE phase change phenomena. For example, the present results are compared with the analytical solutions by Stefan or Neumann problems, and the effect of the thermal properties on the interfacial moving feature can be studied. And also, one-dimensional unsteady heat conduction equation for the transient solidification problem should be solved numerically for the detailed examination. In addition, the crystal structure and dendrite formation of the solid LBE could be visualized by the present method. For further understanding, the crystal structure analysis will be done and recrystallization of the LBE is analyzed quantitatively.

References

- Agostini, P., Baicchi, E., Zucchini, A. and Benamati, G., 2004. The re-crystallization issue in lead-bismuth technology, *Journal of Nuclear Materials*, 335, 275–279,
- Khairulin, R.A., Lyapunov, K.M., Mozgovoï, A.G. and Stankus, S.V., 2005. Crystallization and relaxation phenomena in the bismuth-lead eutectic, *Journal of Alloys and Compounds*, 387, 183–186,
- Nuclear Energy Agency, 2015. Handbook on Lead-bismuth Eutectic Alloy and Properties, Materials Compatibility, Thermal-hydraulics and Technologies, NEA. No. 7268, OECD/NEA, Paris,
- Sato, H., Kamiyama, T. and Kiyonagi, Y., 2011. A rietveld-type analysis code for pulsed neutron Bragg-edge transmission imaging and quantitative evaluation of texture and microstructure of a welded α -iron plate, *Materials Transactions*, 52-6, 1294–1302,
- Takada, O., Kamiyama, T. and Kiyonagi, Y., 2010. Study on phase transition of Pb-Bi eutectic alloy by neutron transmission spectroscopy, *Journal of Nuclear Materials*, 398, 129–131,
- Zhang, J., 2014. Lead-bismuth eutectic (LBE): A coolant candidate for Gen. IV advanced nuclear reactor concepts, *Advanced Engineering Materials*, 16, 349–356,
- Zucchini, A., Agostini, P. and Baicchi, E., 2005. Lead-bismuth eutectic recrystallization studies for the Megapie target, *Journal of Nuclear Materials*, 336, 291–298,